Desalination and Water Treatment
www.deswater.com

doi: 10.5004/dwt.2018.21877

108 (2018) 207–215
March

Defluoridation of water by wasted red brick paving blocks

Tahir Rafique[a,*], Muhammad Anas[a,b], Khalid Mehmood Chadhar[a,c], Faisal Soomro[b], Sofia Khalique Alvi[a]

[a]*Applied Chemistry Research Centre, PCSIR Laboratories Complex, Karachi – 75280, Pakistan, Tel. +92 333 3564570; Fax: +92 21 99261947; emails: tahirrafique92@yahoo.com (T. Rafique), muhammadanas_raza@yahoo.com (M. Anas), khalid.mehmood@pgjdc.org (K.M. Chadhar), sofiaalvi@yahoo.com (S.K. Alvi)*
[b]*Department of Chemistry, University of Karachi, Karachi, Pakistan, email: fezzsumro@yahoo.com*
[c]*Institute of Advanced Research Studies in Chemical Sciences, University of Sindh, Jamshoro*

Received 9 May 2017; Accepted 29 December 2017

ABSTRACT

This study assesses the fluoride adsorption characteristics of red brick paving blocks or red pavers which is locally available and a cheap potential adsorbent for defluoridation. Batch experiments were conducted to evaluate basic parameters such as pH, contact time, dosage, and adsorbent capacity. The adsorption data were incorporated with kinetics (Lagergren pseudo-orders) and isotherm models (Langmuir, Freundlich, Dubinin–Radushkevich [DR], and Temkin) to comprehend the mechanism and types of adsorption. The data recorded in the study agreed with the applied models. The mechanism of interaction between red paver and fluoride was of complex nature as Freundlich and DR isotherm models suggest that adsorption is physisorption with little ion exchange mechanism while Lagergren's pseudo-second order kinetics and Langmuir isotherm model outlined that adsorption could be chemisorption. The highest percentage of fluoride removal was achieved at pH range of 6–7 with 62% removal. Elemental and mineral phases on red paver before adsorption were characterized by X-ray diffraction and wavelength dispersive X-ray fluorescence and WD-XRF, major elemental and mineral components were CaO, Fe_2O_3, SiO_2 and Al_2O_3 and ankerite, dolomite, calcite, and lime, respectively.

Keywords: Fluoride; Fluorosis; Paving blocks; Adsorption; Defluoridation

1. Introduction

Fluoride is the anionic form of the highly reactive element fluorine, which is naturally found as part of numerous minerals. Several hydrogeologic processes release fluoride into groundwater which elevates fluoride levels in regional groundwater systems [1–3]. Fluoride is an important micronutrient for humans as it prevents dental caries and facilitates the mineralization of hard tissues [4]. As per the WHO guidelines, the maximum permissible limit of fluoride in drinking water is 1.5 ppm [5]. Elevated levels of fluoride in groundwater could be a serious matter of concern for human health [6,7]. It has become a fact that fluoride is the main cause of dental and skeletal fluorosis which are irreversible changes in teeth and bones, respectively, having no cures to date [8]. The literature on fluoride also reports that it interferes with synthesis of DNA and metabolism of various bio-molecules [9,10]. High fluoride in groundwater is a global problem with WHO estimating that more than 260 million people living all over the world consume water with undesirable fluoride concentration [11]. Occurrences of dental and skeletal fluorosis due to consumption of high fluoride has been reported from several countries of the world such as Pakistan, India, China, Japan, Sri Lanka, Iran, Turkey, Algeria, Mexico, Korea, Italy, Brazil, Malawi, Jordan, Ethiopia, Canada, Norway, Ghana, and Kenya [6,12–14]. Among these countries, rift valley nations are the most afflicted from where the highest known concentration of fluoride in the groundwater has been reported as in Lake Nakuru, Kenya, 2,800 mg/L [15].

* Corresponding author.

Groundwater resources of Thar Desert areas of Sindh province, Pakistan, have also been identified as containing high fluoride concentrations and the inhabitants are consuming groundwater with F^- concentrations as high as 44 mg/L. Since fluorosis is untreatable and the only prevention is to consume water that has fluoride concentration below the maximum permissible limit, it becomes indispensable to treat water to bring fluoride levels to the desirable limit. For the purpose of removing fluoride from drinking water to bring it under the WHO recommended limit, a number of techniques have been developed which includes, membrane processes such as reverse osmosis membrane process, dialysis and electrodialysis, adsorption techniques, synthetic resins, and biopolymers [16]. Among these techniques, adsorption is the most extensively applied technique because of its simplicity, rapidity, low operating cost, and the ability to regenerate adsorbents for reuse. Several classes of materials have been proposed for the adsorption of fluoride such as alumina and aluminum-based adsorbents, bauxite, red mud, clays, soils, and carbon-based materials are to name some [17]. Red brick paving blocks are used as a paving material for the exterior flooring and are manufactured in high compression machine using concrete materials such as Portland cement, fine aggregate, and crushed aggregate. Sometimes few typically selected admixtures such as calcium chloride, marble dust, barite, kiln dust, ground limestone, brick powder, calcium stearate, etc., are used for improving the properties of concrete. It is estimated that Karachi alone has a daily demand of 0.5 million prefabricated construction blocks, such as solid blocks, hollow blocks, pavers, and kerbstones [18] which subsequently generates a huge amount of solid waste material that can be utilized for the defluoridation purpose. In the present study, the potential of red paver (RP) was evaluated for removal of fluoride from aqueous media through batch experiment. Furthermore, kinetics studies were carried out to understand the mechanism of adsorption and parameters such as adsorbent dose, adsorbate concentration, pH, and contact time were also optimized.

2. Materials and methods

2.1. Conditioning of red paver

RPs used in this study were collected randomly from the local market without any chemical treatment, where RPs are commonly used for construction purposes. The RPs were crushed to increase the surface area and then sieved mechanically to get uniform sized particles of RPs for experiments. The sieved RPs were washed multiple times with de-ionized water to remove the fine dust, and then filtered and oven dried at 105°C for use in experiments.

2.2. Reagents

All the reagents used were of AR grade. Fluoride stock solution of 1,000 mg/L was prepared by dissolving 2.21 g anhydrous sodium fluoride in 1-L volumetric flask with de-ionized water. All the working standards were prepared by proper dilution of stock solution with de-ionized water. Total ionic strength adjustment buffer (TISAB-IV) solution was prepared by dissolving 58 g of sodium chloride, 57 mL of glacial acetic acid and approximately 150 mL of 6 M NaOH in a volume of 1,000 mL. The pH was initially adjusted to the selected values with dilute HCl and NaOH solutions.

2.3. Instrumentation and mode of analysis

A pre-determined amount of uniformly sized RP particles was added into 100 mL conical flask containing a specific volume of the known initial concentration of fluoride solution. The mixture was agitated using orbital shaker at constant rpm and specific interval of time. Thereafter the mixture was filtered using Whatman # 41 filter paper. The fluoride concentration and pH of the adsorbate samples were determined by using Thermo Scientific Orion 5-Star pH/ISE/DO/conductivity meter. To maintain the pH of the solution at 6 and to eliminate the interference of complexing ions, samples were diluted in 1:1 ratio with TISAB-IV solution before analysis. The fluoride ion selective electrode was calibrated prior to each experiment to determine the slope and intercept of the electrode. The pH electrode was also calibrated using pH calibration buffers whenever the measurements were made. Temperature-controlled orbital shaker, Model IST-3075R made Jeio Tech, South Korea, was used for batch mode adsorption studies.

2.4. Batch adsorption equilibrium studies

The batch mode adsorption experiment was conducted at ambient temperature, 150 rpm and particle size of 250 μm size to study the effect of variables such as solution pH, adsorbent dosage, contact time, and initial concentration of fluoride on the defluoridation.

Equilibrium time was optimized by taking 1.0 g RP particles and 10 mg/L initial fluoride solution, shaken for the different intervals of time from 10 to 120 min. The adsorption capacity of RP particles was established using 1–6 g of adsorbent (RP particles) shaken with 10 mg/L initial fluoride concentration at equilibrium time. Effect of adsorbate concentration on fluoride removal capacity of RP was demonstrated using 5–50 mg/L initial fluoride concentration at a constant dose of adsorbent. Effect of pH on defluoridation by RP particle was studied between pH 3.0 and 12.0.

The amount of fluoride (mg) adsorbed per unit mass of the adsorbent (g) was calculated from Eq. (1):

$$q = \left(\frac{C_i - C_e}{m} \right) V \tag{1}$$

where q is the fluoride adsorbed (mg/g), C_i is the initial concentration of fluoride (mg/L), C_e is the concentration of fluoride in solution at equilibrium time (mg/L), V is the adsorbate volume (L), and m is the mass of adsorbent (g).

2.5. XRF and XRD analysis

The X-ray fluorescence (XRF) spectrophotometer (Bruker AXS S4 Pioneer) was used to determine the elemental profile of the adsorbent. Phase and mineral identification was done by Siemens D5000 powder diffractometer (X-ray diffraction (XRD)) from 10° to 90° 2θ using a step size of 0.05°/s.

Identification was evaluated with the help of the Diffrac^{pus} searching software version 7.0.108 by comparing the data (peaks and relative intensities) with peaks and relative intensities from a very large set of "standard" data provided by the International Center for Diffraction Data.

3. Results and discussion

3.1. Characterization of adsorbent

3.1.1. Elemental analysis

Results of XRF analysis of red pavers along with oxides form of the elements, and their quantities in percentage have been given in Table 1. Major elements in oxide form were CaO (60.64%), SiO_2 (23.60%), Fe_2O_3 (7.45%), and Al_2O_3 (4.13%). The oxides/hydroxides of these metals have a high affinity for fluoride and favor the ion exchange mechanism [19,20].

3.1.2. Mineral phase analysis

Mineral phases, their formulae, and percentages have been given in Table 2. Major minerals in the composition of red pavers were dolomite (73.90%), lime (10.80%), calcite (7.30%), and ankerite (5.20%).

Table 1
Elemental chemical composition (oxide form) of red brick paving block sample by XRF technique

Elemental composition	%
SiO_2	23.600
Al_2O_3	4.130
Fe_2O_3	7.458
CaO	60.640
K_2O	0.526
MgO	0.992
Na_2O	0.445
TiO_2	0.488
Cl	0.034
SO_3	0.775
P_2O_5	0.559

Table 2
Phase and mineral identification of RP sample by XRD technique

Compound name	Formula	Quantities (%)
Ankerite	$Ca(Mg_{0.67}Fe_{0.33}^{+2})(CO_3)_2$	5.2
Dolomite	$CaMg_{0.77}Fe_{0.23}(CO_3)_2$	73.9
Calcite	$CaCO_3$	7.3
Lime	CaO	10.8

3.2. Batch mode adsorption studies

3.2.1. Equilibrium time

The effect of contact time on percentage removal of fluoride is shown in Fig. 1 and it is observed that optimum contact time to remove maximum fluoride (i.e., 62.7%) is 110 min. The data demonstrate that the adsorption of fluoride ion by RP is faster in the first 50 min and equilibrium is established in 110 min after which the curve tends to become linear and may approach the saturation which reflects the monolayer coverage. It could be suggested that during the initial stage of adsorption, many vacant surface sites were available for adsorption. However, as the experiment proceeds, the remaining vacant surface sites are difficult to be occupied due to repulsive forces between the adsorbed F^- on the solid surface and the bulk phase.

3.2.2. Equilibrium pH

Adsorption of F^- onto RP was studied in the pH range of 3–12 and the results are shown in Fig. 2. The results showed that adsorption was maximum (i.e., 62.7%) in the pH range of 6–7 which is consistent with results obtained by other researchers [20–22]. The adsorption is probably favored by low pH since anion adsorption is coupled with the release of OH^- ions. In the acidic pH range, the amount of fluoride adsorbed is slightly decreased and this can be attributed to the formation of weak hydrofluoric acid [23]. In the alkaline pH range, there is a sharp drop in adsorption, which may be due to the competition of the hydroxyl ions with the fluoride for adsorption onto the oxides present in RP [24].

3.2.3. Equilibrium concentration

The effect of initial fluoride concentration on adsorption capacity mg/g and percent adsorption is also shown in Fig. 3. With an increase in fluoride concentration, percentage fluoride adsorption decreases whereas the amount of fluoride adsorbed per fixed mass of adsorbent increases. This indicates that the adsorbent surface offers a limited number of active sites compared with the relatively large number of

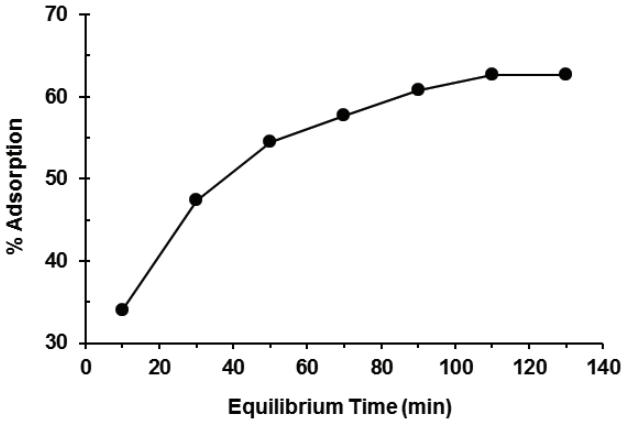

Fig. 1. Effect of equilibrium time on the percentage adsorption at different time intervals (adsorbent dose = 1 g, adsorbate concentration = 10 mg/L, pH = 7).

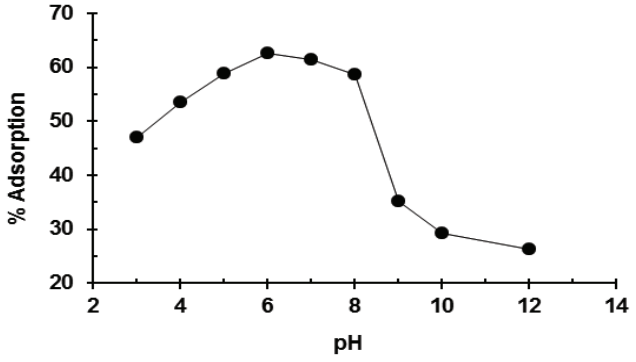

Fig. 2. Effect of pH on the percent adsorption as a function of pH of adsorbate (initial concentration of fluoride = 10 mg/L, adsorbent dose = 1 g, contact time = 110 min).

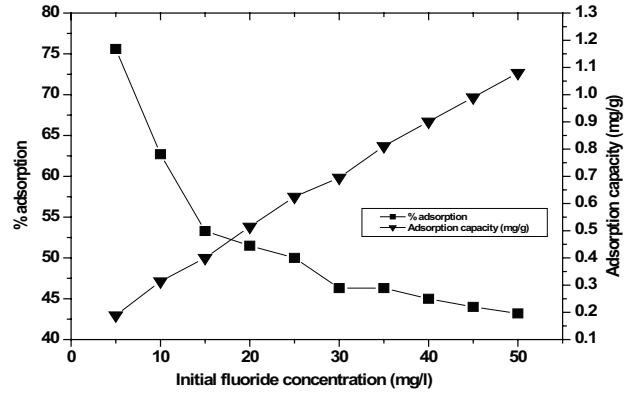

Fig. 3. Plot of amount of fluoride adsorbed per gram of adsorbent and the percentage of fluoride adsorption on adsorbent as a function of initial fluoride concentration (adsorbent dose = 1 g, contact time = 110 min, pH = 7).

active sites required for the high initial fluoride concentration [25]. Adsorption capacity was found to be of the order of 0.19–1.08 mg/g of adsorbent.

3.2.4. Adsorbent dose

The effect of adsorbent dosage on adsorption capacity and percentage removal of RP at optimized pH and initial fluoride concentration is shown in Fig. 4(a) and it indicates that percentage fluoride removal increases, and adsorption capacity decreases as the adsorbent dose is increased. The percentage removal of fluoride increased with an increase in adsorbent dose and nearly 91.0% of fluoride was adsorbed with 6.0 g of adsorbent. However, an adsorbent dose of 1.0 g was optimized for the further study because, after 1.0 g adsorbent dose, the adsorption capacity did not seem to decrease that sharply. An adsorption capacity of 0.31 mg/g and percentage F^- removal of 62% was achieved at an optimized dose of 1.0 g.

Distribution coefficient K_d reflects the binding ability of the surface for ions and is dependent on pH and type of surface. Fig. 4(b) shows plot of K_d values as a function of adsorbent dose. Initially, K_d values decrease sharply and then it

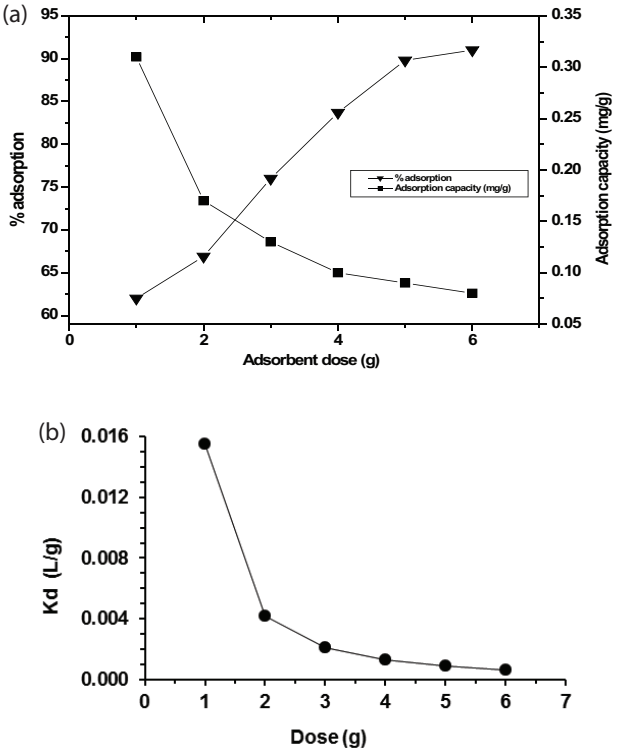

Fig. 4. (a) Plot of amount of fluoride adsorbed per gram of adsorbent and the percentage of fluoride adsorption on adsorbent as a function of adsorbent dose (initial fluoride concentration = 10 mg/L, contact time = 110 min, pH = 7). (b) Plot of distribution coefficient as a function of adsorbent dose (initial fluoride concentration = 10 mg/L, contact time = 110 min, pH = 7).

approaches linearity (i.e., no significant change) which reflects the homogeneous nature of RP surface [26].

The distribution coefficient values were calculated using Eq. (2):

$$K_d = \frac{C_e}{C_i} \times \frac{V}{m} \tag{2}$$

where K_d is distribution coefficient, C_i is the initial concentration of fluoride (mg/L), C_e is the concentration of fluoride in solution at equilibrium time (mg/L), V is the adsorbate volume (L), and m is the mass of adsorbent (g).

3.3. Kinetics of adsorption

To clarify the adsorption kinetics of fluoride onto RP, two kinetic models Lagergren's pseudo-first order and pseudo-second order models were applied to the experimental data. The kinetics of adsorption of fluoride by red brick was carried out and the plotted results were shown in Fig. 5. The adsorption kinetics is very fast, that is, in the first 50 min most of the fluoride is adsorbed. With further increase in time, a slight increase in adsorption is observed up to about 110 min after which it is essentially constant. Adsorption probably takes place on the surface only with very little diffusion taking place into the pores.

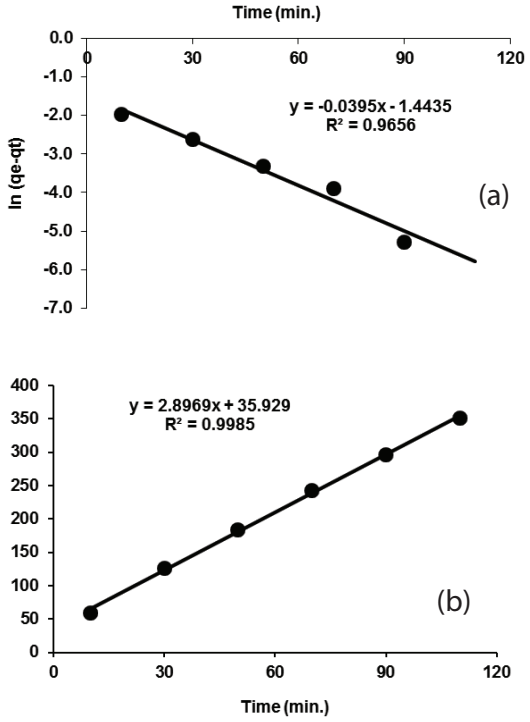

Fig. 5. (a) Plot of Lagergren's pseudo-first order and (b) pseudo-second order models (initial concentration of fluoride = 10 mg/L, adsorbent dose = 1 g, pH = 7).

The pseudo-first order model assumes that the fluoride ion only adsorbs on one adsorption site of the adsorbent surface and is represented as Eq. (3):

Linear form of pseudo-first order is:

$$\ln(q_e - q_t) = q_{lm} - kt \tag{3}$$

where q_e and q_t (mg/g) are adsorption capacities at equilibrium and specific interval of time t (min), q_{lm} is the Lagergren maximum adsorption capacity (mg/g) and k (min^{-1}) is the rate constant.

On the other hand, the essential assumption of the pseudo-second order model is that one target ion is adsorbed onto two surface sites. Linear form of pseudo-second order is represented as Eq. (4):

$$\frac{t}{q_t} = \frac{1}{k_2 q_e} + \frac{t}{q_e} \tag{4}$$

where q_e and q_t (mg/g) are adsorption capacity at equilibrium and specific interval of time t (min), and k_2 is the pseudo-second order rate constant (g/mg min).

Table 3 lists the results of rate constant studies for fluoride ion in single combination by the pseudo-first order and pseudo-second order models. The value of correlation coefficient R^2 for the pseudo-second order adsorption model is relatively high (0.999), and the adsorption capacities calculated by the model (0.345 mg/g) are also close to those determined by experiments (0.314 mg/g; Fig. 3).

Table 3
Comparison between adsorption kinetic parameters and coefficients of correlation associated to the Lagergren's pseudo-first order and pseudo-second order kinetic (initial fluoride concentration = 10 mg/L, adsorbent dose = 1 g, pH = 7)

Adsorption kinetic models	Parameters	Values
Lagergren's pseudo-first-order kinetic model	R^2	0.966
	k (min^{-1})	0.0395
	q_{lm} (mg/g)	0.236
Lagergren's pseudo-second-order kinetic model	R^2	0.999
	k_2 (g/mg min)	0.081
	q_e (mg/g)	0.345

However, the value of R^2 for the pseudo-first order model was 0.966 but value of adsorption capacities is not much satisfactory, that is, 0.236 mg/g (Table 3). Therefore, it has been concluded that the pseudo-second order adsorption model is more suitable to describe the adsorption kinetics of fluoride ion over RP. This suggests that the rate limiting step in this adsorption process may be chemisorption and there is an involvement of valent forces by the sharing or exchange of electrons between adsorbent and adsorbate [27].

3.4. Adsorption isotherms

Adsorption isotherms are the prerequisite parameters to understand the behavior of the adsorption process. Along with the affinity of an ion for adsorption, the shape of an isotherm also reflects the possible mode of adsorption. It also expresses the relation between the mass of adsorbate at the solid and liquid phase at particular temperature [28]. Understanding of the sorption capacities of adsorbent materials, such as RP, facilitates to design and develop treatment systems for particular adsorbate systems [29]. The adsorption isotherms data correlated with the linear form of the Langmuir, Freundlich, DR, and Temkin adsorption isotherm models for fluoride onto the RP are shown in Fig. 6, whereas Table 4 shows the coefficients of determination (R^2) and the isotherm constants of the Freundlich, Langmuir, DR, and Temkin equations in the single system.

3.4.1. Langmuir adsorption isotherm

A basic assumption of the Langmuir model is that adsorption takes place at specific sites within the adsorbent surface. Theoretically, therefore, a saturation value is reached beyond which no further adsorption can take place. The Langmuir isotherm suggests monolayer coverage of adsorbate over a homogenous adsorbent surface [30]. The data obtained from the adsorption experiment conducted in the present investigation was fitted in the linear expression Langmuir isotherm (Eq. (5)):

$$\frac{C_t}{q_e} = \frac{1}{K_L Q_{\max}} + \frac{C_t}{Q_{\max}} \tag{5}$$

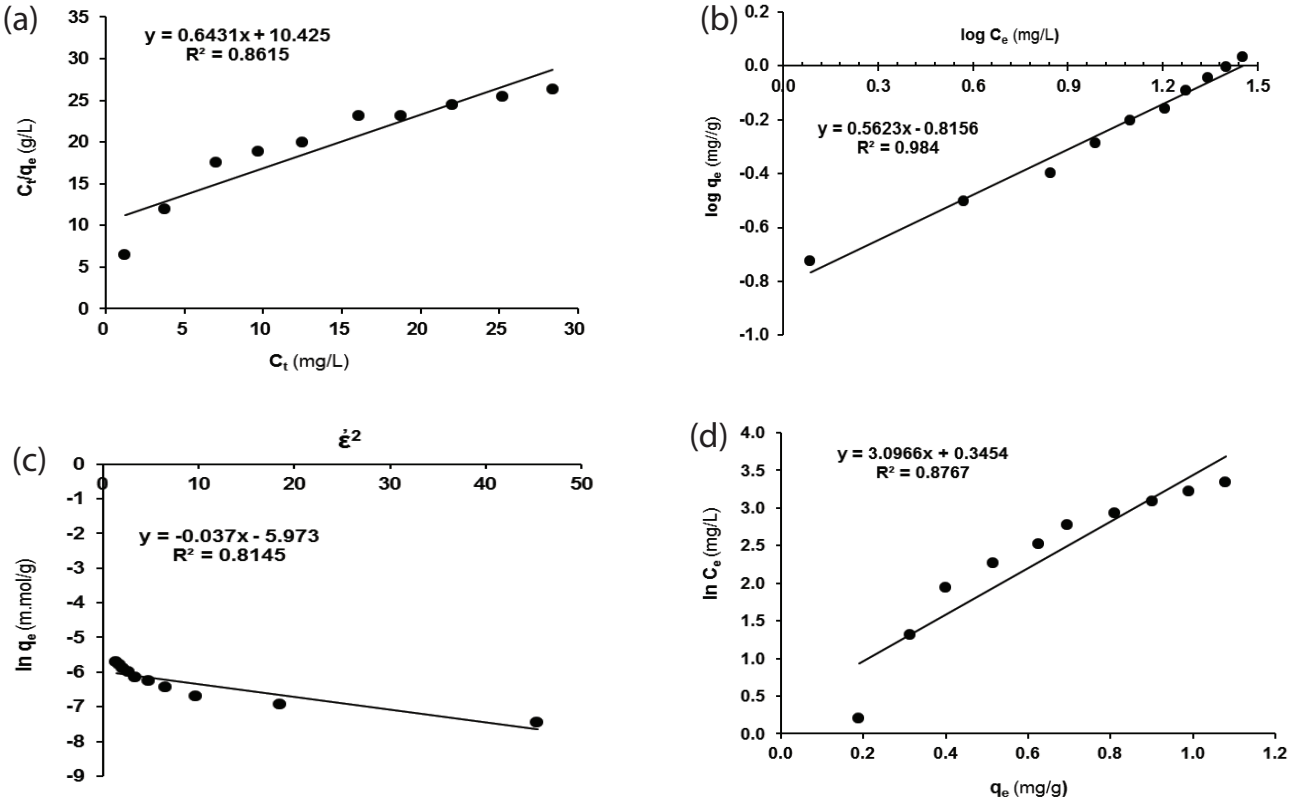

Fig. 6. (a) Plots of Langmuir adsorption isotherm, (b) Freundlich adsorption isotherm, (c) DR isotherm and (d) Temkin isotherm (initial concentration of fluoride = 10 mg/L, adsorbent dose = 1 g, contact time = 110 min, pH = 7).

Table 4
Langmuir, Freundlich, Dubinin–Radushkevich, and Temkin isotherm constants for the adsorption of fluoride ion on RP adsorbent (initial fluoride concentration = 10 mg/L, contact time = 110 min, adsorbent dose = 1 g, pH = 7)

Isotherms	Parameters	Values
Langmuir	R^2	0.862
	K_L	16.211
	Q_{max}	1.555
	R_L	(0.013–0.114)
Freundlich	R^2	0.984
	K_F	0.153
	$1/n$	0.562
	n	1.778
DR equation constants	R^2	0.955
	β_D	0.0370
	q_m	0.0025
	E (kJ/mol)	8.602
Temkin	R^2	0.877
	β_T	3.097
	K_T	1.118

Here K_L is Langmuir constant and Q_{max} theoretical monolayer capacity, and their values were evaluated by slope and intercept of the linear plot of C_t/q_e against C_t (Fig. 6(a)). The Langmuir equation is applicable to homogeneous adsorption where the adsorption of each molecule has equal adsorption activation energy.

Table 4 presents the values of the parameters introduced by the Langmuir isotherm, as observed from Table 4, the correlation of the Langmuir isotherm was performed with the fluoride adsorption data onto the RP. The feasibility of the Langmuir isotherm can be expressed in terms of a dimensionless constant, separation factor or equilibrium parameter, R_L, which is defined as Eq. (6) [31]:

$$R_L = \frac{1}{\left(1 + bC_i\right)} \tag{6}$$

where b is the Langmuir constant and C_i is the initial concentration of the metal ions. R_L values between 0 and 1 indicate favorable adsorption while $R_L > 1$ is unfavorable. From our study, R_L values for fluoride ion adsorption ranged from 0.013 to 0.114 which indicates that the adsorption process is favorable.

3.4.2. Freundlich isotherm

The Freundlich model is used for heterogeneous surfaces, with different sorption energies. Freundlich expression is an

exponential equation and assumes the multilayer coverage of the adsorbent surface. Theoretically, using the following expression (Eq. (7)), an infinite amount of adsorption can occur [32].

$$q_e = K_F C_e^{\frac{1}{n}} \tag{7}$$

where K_F and $1/n$ are the Freundlich constants. The constants K_F and $1/n$ were obtained by slope and intercept of the linear form of the equation as shown below in Eq. (8):

$$\ln q_e = \ln K_F + \frac{1}{n}\ln C_e \tag{8}$$

Plotting $\ln q_e$ vs. $\ln C_e$ (Fig. 6(b)) results in a straight line of slope $1/n$ and intercept $\ln K_F$ and the value of the linear regression coefficient (R^2) was found to be 0.984, indicating that the data substantially fits in the model. The values of K_F and $1/n$ calculated from Fig. 6(b) were found to be 0.141 and 2.078, respectively, (Table 4).

The degree of non-linearity between solution concentration and adsorption depends upon the value of n as follows: if the value of n is equal to unity, the adsorption is linear; a value below unity implies that adsorption process is chemisorption; if the value is above unity then adsorption is a favorable physical process [33]. The value of n in this study has been found to be greater than unity, that is, 1.779 (Table 4) which shows that adsorption process of fluoride onto the RP adsorbent is fairly physisorption.

3.4.3. Dubinin–Radushkevich equation

Dubinin–Radushkevich (DR) equation was widely used to express the adsorption isotherms in micropores and was selected for present study to estimate the characteristics porosity of the RP and the apparent energy of adsorption [34]. The model is represented as Eq. (9):

$$q_e = \beta_T \ln K_T + \beta_T \ln C_e \tag{9}$$

where β_D is related to the free energy of adsorption per mole of the adsorbate as it migrates to the surface of the adsorbent from infinite distance in the solution and q_m is the DR isotherm constant related to the degree of adsorbate adsorption by the adsorbent surface. The linear form of above equation is given as Eq. (10):

$$\ln q_e = \ln q_m - \beta_D \left\{ RT \ln\left(1 + \frac{1}{c_e}\right)\right\}^2 \tag{10}$$

or

$$\ln q_e = \ln q_m - \beta_D \acute{\varepsilon}^2 \tag{11}$$

here, (Polanyi Potential) $\acute{\varepsilon} = RT \ln\left(1 + \frac{1}{c_e}\right)$ (12)

A plot of $\ln q_e$ against $\acute{\varepsilon}^2$ (Fig. 6(c)) indicates a good agreement between the isotherm model and the experimental data. The values of q_m and β_D calculated from the intercepts and slopes of the plots (Fig. 6(c)) are shown in Table 4 with the apparent energy (E) of adsorption from the DR isotherm, which was calculated using Eq. (13):

$$E = \frac{1}{(2\beta_D)^{\frac{1}{2}}} \tag{13}$$

Values of E ranging from 1 to 8 (kJ/mol) represent physisorption, 8–16 (kJ/mol) ion exchange and 16–40 (kJ/mol) represent chemisorption process [35]. The higher the values of q_m, the higher the adsorption capacity. The values of q_m from Table 4 are seen to be higher for RP. The values of the apparent energy of adsorption shown in Table 4 depict physisorption process with little ion exchange mechanism [36].

3.4.4. Temkin isotherm

Temkin and Pyzhev considered the effect of some indirect adsorbate/adsorbate interaction on adsorption isotherms and suggested that because of interaction the heat of adsorption of all the molecules in the layer would decrease linearly with coverage [37]. The amount of adsorbate can be given as Eq. (14):

$$q_e = \beta_T \ln K_T + \beta_T \ln C_e \tag{14}$$

where K_T is the equilibrium binding constant (L/mg) corresponding to maximum binding energy and β_T is a Temkin isotherm factor related to the heat of the adsorption and is given by:

$$\beta_T = \frac{RT}{b} \tag{15}$$

Here, b is related to heat of adsorption (J/mol), R is the gas constant (8.314 J/mol K), and T is the absolute temperature (K).

Plotting q_e vs. $\ln C_e$ (Fig. 6(d)) resulted in a little deviated straight line of slope β_T and intercept K_T, which shows the applicability of the Temkin model for adsorption of fluoride ion onto the RP adsorbent. The Temkin isotherm constants, K_T, β_T, and R^2 are presented in Table 4.

4. Conclusion

The study focused on the applicability of a new adsorbent RP for removal of fluoride from aqueous solution in single ion systems. The adsorption process was described well by the Langmuir and Freundlich isotherm equations. The maximal adsorption efficiency of the RP has been found to be 62% at optimized conditions. Results showed that the percentage of fluoride removal is a function of adsorbent dose and contact time at a given initial fluoride concentration. It increased with time and adsorbent dose. Kinetically, the adsorption process was favored by the pseudo-second order model and

was found to occur in about 40 min with reasonable activation energy and rate. The Langmuir, Freundlich, DR, and Temkin isotherm adsorption models were applied on batch experiments data and have been found reasonably well. The values of dimensionless equilibrium parameter (R_L) at different concentrations indicate the favorability of the process described in the present study. On the basis of the above information it is difficult to explain the mechanism of adsorption. The applicability of pseudo-second-order kinetics and Langmuir isotherm model outlines adsorption could be chemisorption involving valent forces through the sharing or exchange of electrons between adsorbate and adsorbent. Whereas Freundlich model and mean free energy (i.e., 8.602 kJ/mol) by DR model suggest physisorption process with little ion exchange mechanism, hence it can be concluded that adsorption process for proposed study is complex in nature. There is an involvement of both valent forces as well as van der wall forces between adsorbents (RP) and fluoride. Overall process was dominated by physisorption mechanism. The analyses by XRF and XRD showed that the adsorbent had major elemental oxides of CaO, SiO_2, Fe_2O_3, and Al_2O_3 while the major mineral phases were found to be dolomite, lime, calcite, and ankerite.

Acknowledgment

The authors are highly thankful to Pakistan Science Foundation for financial support of this research under Project Nos. PSF/RES/S-PCSIR/Envr (86) and PSF/R&D/ILP/039/10.

References

[1] S. Ayoob, A.K. Gupta, Fluoride in drinking water: a review on the status and stress effects, Crit. Rev. Environ. Sci. Technol., 36 (2006) 433–487.
[2] B.K. Handa, Geochemistry and genesis of fluoride-containing ground waters in India, Groundwater, 13 (1975) 275–281.
[3] D.L. Ozsvath, Fluoride and environmental health: a review, Rev. Environ. Sci. Biotechnol., 8 (2009) 59–79.
[4] D.O. Mullane, R. Baez, S. Jones, M. Lennon, P.E. Petersen, A. Rugg-Gunn, H. Whelton, G. Whitford, Fluoride and oral health, Community Dent. Health, 33 (2016) 69–99.
[5] WHO, Guidelines for Drinking-Water Quality, in: Recommendations, World Health Organization, Geneva, 2004, p. 376.
[6] M.T. Alarcon-Herrera, I.R. MartIn-Dominguez, R. Trejo-Vázquez, S. Rodriguez-Dozal, Well water fluoride, dental fluorosis, and bone fractures in the Guadiana Valley of Mexico, Fluoride, 34 (2001) 139–149.
[7] S. Jolly, B. Singh, O. Mathur, K. Malhotra, Epidemiological, clinical, and biochemical study of endemic dental and skeletal fluorosis in Punjab, Br. Med. J., 4 (1968) 427–429.
[8] A.K. Susheela, Epidemiological Studies of Health Risks from Drinking Water Naturally Contaminated with Fluoride, IAHS Publications, Series of Proceedings and Reports, International Association of Hydrological Sciences, Vol. 233, 1995, pp. 123–134.
[9] L.-F. He, J.-G. Chen, DNA damage, apoptosis and cell cycle changes induced by fluoride in rat oral mucosal cells and hepatocytes, World J. Gastroenterol., 12 (2006) 1144–1148.
[10] O. Barbier, L. Arreola-Mendoza, L.M. Del Razo, Molecular mechanisms of fluoride toxicity, Chem. Biol. Interact., 188 (2010) 319–333.
[11] WHO, Health Criteria and Other Supporting Information, in: Guidelines for Drinking Water Quality, Geneva, 1984.
[12] T. Rafique, I. Ahmed, F. Soomro, M.H. Khan, K. Shirin, Fluoride levels in urine, blood plasma and serum of people living in an endemic fluorosis area in the Thar Desert, Pakistan, J. Chem. Soc. Pak., 37 (2015) 1223–1230.
[13] A. Baba, G. Tayfur, Groundwater contamination and its effect on health in Turkey, Environ. Monit. Assess., 183 (2011) 77–94.
[14] S. Teotia, M. Teotia, R. Singh, Hydro-geochemical aspects of endemic skeletal fluorosis in India – an epidemiologic study, Fluoride, 14 (1981) 69–74.
[15] R. Tekle-Haimanot, Z. Melaku, H. Kloos, C. Reimann, W. Fantaye, L. Zerihun, K. Bjorvatn, The geographic distribution of fluoride in surface and groundwater in Ethiopia with an emphasis on the Rift Valley, Sci. Total Environ., 367 (2006) 182–190.
[16] M. Mohapatra, S. Anand, B.K. Mishra, D.E. Giles, P. Singh, Review of fluoride removal from drinking water, J. Environ. Manage., 91 (2009) 67–77.
[17] A. Bhatnagar, E. Kumar, M. Sillanpää, Fluoride removal from water by adsorption—a review, Chem. Eng. J., 171 (2011) 811–840.
[18] SMEDA-Sindh (Small and Medium Enterprises Development Authority), Pre-Feasibility Study (Pre-fabricated Construction Blocks), Government of Sindh, Ministry of Industries & Production, Document Number PREF-NO: 13, Lahore, 2016, pp. 39. Available at: http://www.commerce.gov.pk/wp-content/uploads/2017/05/Pre-Fabricated-Construction-Blocks.pdf.
[19] S. Kagne, S. Jagtap, P. Dhawade, S. Kamble, S. Devotta, S. Rayalu, Hydrated cement: a promising adsorbent for the removal of fluoride from aqueous solution, J. Hazard. Mater., 154 (2008) 88–95.
[20] T. Rafique, K.M. Chadhar, T.H. Usmani, S.Q. Memon, K. Shirin, S. Kamaluddin, F. Soomro, Adsorption behavior of fluoride ion on trimetal-oxide adsorbent, Desal. Wat. Treat., 56 (2015) 1669–1680.
[21] B. Zhao, Y. Zhang, X. Dou, X. Wu, M. Yang, Granulation of Fe-Al-Ce trimetal hydroxide as a fluoride adsorbent using the extrusion method, Chem. Eng. J., 185 (2012) 211–218.
[22] A.M. Raichur, M.J. Basu, Adsorption of fluoride onto mixed rare earth oxides, Sep. Sci. Technol., 24 (2001) 121–127.
[23] S. Meenakshi, P. Anitha Pius, G. Karthikeyan, B.V. Apparao, The pH dependent of efficiency of activated alumina in defluoridation of water, Indian J. Environ. Protect., 7 (1991) 511–513.
[24] P.S.P. Harikumar, C. Jaseela, T. Megha, Defluoridation of water using biosorbents, Nat. Sci., 4 (2012) 245–251.
[25] S.S. Dash, M.K. Sahu, E. Sahu, R.K. Patel, Fluoride removal from aqueous solutions using cerium loaded mesoporous zirconium phosphate, New J. Chem., 39 (2015) 7300–7308.
[26] A.E. Yilmaz, B.A. Fil, K. Karcioglu, A new adsorbent for fluoride removal: the utilization of sludge waste from electrocoagulation as adsorbent, Global NEST J., 17 (2015) 186–197.
[27] M. Arshadi, M.J. Amiri, S. Mousavi, Kinetic, equilibrium and thermodynamic investigations of Ni (II), Cd (II), Cu (II) and Co (II) adsorption on barley straw ash, Water Resour. Ind., 6 (2012) 1–17.
[28] R. Arunachalam, G. Annadurai, Nano-porous adsorbent from fruit peel waste for decolorization studies, Res. J. Environ. Sci., 5 (2011) 434–443.
[29] P. Velmurugan, V. Rathinakumar, G. Dhinakaran, Dye removal from aqueous solution using low cost adsorbent, Int. J. Environ. Sci., 1 (2011) 1492–1503.
[30] A.O. Dada, A.P. Olalekan, A.M. Olatunya, O. Dada, Langmuir, Freundlich, Temkin and Dubinin-Radushkevich isotherms studies of equilibrium sorption of Zn^{2+} unto phosphoric acid modified rice husk, J. Appl. Chem., 3 (2012) 38–45.
[31] N. Ahalya, R.D. Kanamadi, T.V. Ramachandra, Biosorption of chromium (VI) from aqueous solutions by the husk of Bengal gram (*Cicer arientinum*), Electron. J. Biotechnol., 8 (2005) 258–264.
[32] B. Ismail, S.T. Hussain, S. Akram, Adsorption of methylene blue onto spinel magnesium aluminate nanoparticles: adsorption isotherms, kinetic and thermodynamic studies, Chem. Eng. J., 219 (2013) 395–402.

[33] P.S. Kumar, S. Ramalingam, C. Senthamarai, M. Niranjanaa, P. Vijayalakshmi, S. Sivanesan, Adsorption of dye from aqueous solution by cashew nut shell: studies on equilibrium isotherm, kinetics and thermodynamics of interactions, Desalination, 261 (2010) 52–60.
[34] A.U. Itodo, H.U. Itodo, Sorption energies estimation using Dubinin-Radushkevich and Temkin adsorption isotherms, Life Sci., 7 (2010) 31–39.
[35] S. Chien, W. Clayton, Application of Elovich equation to the kinetics of phosphate release and sorption in soils, Soil Sci. Soc. Am. J., 44 (1980) 265–268.
[36] M.J. Horsfall, A.I. Spiff, A.A. Abia, Studies on the influence of mercaptoacetic acid (MAA) modification of cassava (*Manihot sculenta* Cranz.) waste biomass on the adsorption of Cu^{2+} and Cd^{2+} from aqueous solution, Bull. Korean Chem. Soc., 25 (2004) 969–976.
[37] J.M. Salman, K.A. Al-Saad, Adsorption of 2, 4-dichlorophenoxyacetic acid onto date seeds activated carbon: equilibrium, kinetic and thermodynamic studies, Int. J. Chem. Sci., 690 (2012) 677–690.